Food 3D Printing: Effect of Heat Transfer on Print Stability of Chocolate

P Rando, M Ramaioli

Food 3D Printing: Effect of Heat Transfer on Print Stability of Chocolate

P. Rando[a,b], M. Ramaioli[b,*]

[a] *Department of Chemical and Process Engineering, University of Surrey, GU2 7XH, Guildford, UK*

[b] *UMR SayFood, Université Paris-Saclay, AgroParisTech, INRAE, 78850, Thiverval Grignon, France*

Abstract

Food 3D Printing is a novel technology which allows manufacturing three dimensional edible objects with customized shape and structure, by extruding and depositing progressively several layers. The overall process is complex since many phenomena occurs simultaneously: non-Newtonian flows, heat transfer, sintering between different layers and solidification of the printed material after deposition.

This study focuses on the interplay between the rheological and thermal properties of chocolate products, and printing conditions, in order to predict the stability of 3D printed structures. The effect of printing velocity (V_p) and environmental temperature (T_e) on chocolate printed structure was investigated using IR thermography to characterize the local cooling dynamics.

3D edible structures can be manufactured successfully only below a critical print velocity which depends on the environmental temperature. At $T_e = 18°C$, V_p should be lower than 16 mm/s while at $20°C$ lower than 8 mm/s. This conditions ensure a sufficient cooling and solidification of the cocoa butter, which is needed for print stability. A stability criterion based on the local yield stress is proposed to explain the stability or collapse of the 3D printed structures.

The understanding provided by this work can help optimising food 3D printing conditions and product formulation.

Keywords: 3D Printing, Food Design, Chocolate, IR Thermography, Heat Transfer.

Nomenclature

BJ	Binder Jetting
CAD	Computer Aided Design
DSC	Differential Scanning Calorimetry

ICA	International Confectionery Agency
IJ	Inkjet Printing
IR	Infra-red
SLS	Selective Laser Sintering
STL	stereolithography

1. Introduction

In the last decade, additive manufacturing technologies have been employed to produce food with customized shape, structure, flavour, texture, and even to customize the nutritional characteristics [1].

Even though several techniques are available [2], such as Selective Laser Sintering (SLS), Ink-Jet Printing (IJ), Binder Jetting (BJ) and Paste Extrusion, in the last years the latter became more popular due to its versatility and simplicity. In this process, a thin layer of fluid material is deposited onto a platform from an heated nozzles and 3D structures are created layer-by-layer. A rapid rheological transition towards a solid material is sought after deposition. During these steps the material temperature is a key parameter to achieve a successful and stable print [3]. The effect of the temperature due to different printing condition has been investigated during the manufacturing of plastic polymers using thermocouples ([4], [5]) and Infra-Red (IR) thermography [6]. However, food materials may have poorer mechanical properties compared to plastic, which can affect negatively the stability of printed structures.

The 3D printing process might be challenging, especially when it is applied to new materials. In Food 3D Printing, researchers have tested diverse food printing materials, often called inks, such as starch based products ([7], [8]), chocolate ([9], [10]), pectin based foods [11], food gels ([12], [13], [14]), sodium caseinate [15] and more complex products ([16], [17]). Authors often uses a trial and error approach, varying the food composition and looking at the range of viscosity that allows the material to flow through the nozzle. Typically, fluids with a shear-thinning behaviour can easily be extruded at higher shear rate. Schutyser *et al.* [15] and Liu *et al.* used a model based on a modified Poiseuille equation for a Power law fluid, to predict the pressure drops in the nozzle. On the other hand, the yield stress and the elastic modulus are sometimes related to the capability to create self-supporting structures [8]. Moreover, some authors distinguished between material's yield stress at nozzle temperature, which can be used to characterize the flow behaviour and the yield stress at room temperature to investigate the stability of 3D structures [14]. The complex modulus are related to the capability of the material to resist compression stress. Authors investigated the role of the damping factor, the ratio between storage and loss modulus. Printing materials having a higher damping factor show solid-like behaviour and therefore have an higher capability to support a 3D structure ([8], [13]). However, in these studies inks were formulated adding

thickeners and/or gelling agents which drastically increases the value of the yield stress, improving the stability of prints after deposition. On the other hand, often fat-based and/or carbohydrates products show a dramatic change on rheological behaviour when their temperature decreases below the melting or the glass transition temperature [2].

A food material used with a certain degree of success in Paste Extrusion food 3D printing is chocolate [2], because it solidifies after deposition. Chocolate can be defined as a dense suspension of non-fat particles such as sugar, cocoa solids and milk powders, dispersed in a continuous phase of cocoa butter [18]. In the molten state, chocolate presents a shear-thinning behaviour, a yield stress and tixotropy, which can vary depending on its formulation and particle size distribution ([19], [20]). Chocolate shear rheology has been often described with a Casson model, as recommended from International Confectionery Agency (ICA). Nevertheless, Sokmen *et al.* studied the effects of different bulk sweeteners with different particles size distributions on chocolate rheological properties and concluded that the Herschel-Bulkley model is the best model for the chocolate samples considered [21].

Cocoa butter is mainly a mixture of triglycerids: oleic, stearic and palmitic acids [18]. Depending on its composition and the production process it can crystallize in VI different polyformic forms. The melting temperature (T_m) of each crystalline form is different and changes the chocolate texture. Form I is the less stable and melts at 17 $^\circ C$, crystal in forms II, III, IV melts in a temperature range between 22 and 28 $^\circ C$, whereas forms V and VI are the most stable. Typically crystals in the V form ($T_m = 32 - 34^\circ C$) are desired for the production of confectionery products, because they melt inside the mouth.

Few authors have already developed and optimized chocolate 3D printers: Hao *et al.* suggested that the main printing parameters affecting the overall print quality are nozzle velocity, nozzle height and extrusion rate [22], whereas, Lanaro *et al.* [23] described the optimization of several process parameters such as extrusion rate, printing speed and cooling rate and reported that cooling down the chocolate with an air cooler improves the print stability. Mantihal *et al.* studied the effect of shape and internal structure of 3D printed of chocolate structures with texture analysis ([9], [10]). Moreover, the authors investigated the thermal and rheological properties of chocolate to ensure an appropriate nozzle and build plate temperatures, when the printing material is extruded, but the temperature of the chocolate and its cooling were not characterized during printing.

The effect of 3D printing conditions on the heat transfer post deposition has not been considered in detail in the literature and this knowledge gap can in turn limit the 3D printing performance and stability, obliging to working by trial and error when looking for conditions leading to stable prints.

In this study we investigated the interplay between chocolate rheological and heat transfer properties and the 3D printing process parameters. The temperature profiles of a chocolate ink after deposition were measured experimentally, using IR thermography, while investigating the effect of different process conditions, such as printing speed and build temperature, in order to understand

their effect on the ink heat transfer, cooling dynamics and structure stability. The approach developed in this study can be used to identify optimal 3D printing process conditions or to guide the formulation of food inks whenever cooling induce a strong change in rheological properties.

2. Materials and Methods

2.1. Materials

The chocolate BC-811 (Barry Callebaut, UK) was used as 3D printing ink. It is a dark chocolate in form of callets, which contains 37.8% fat and 54.5% cocoa solids.

Chocolate callets were melted and tempered with a Mini Rev Tempering Machine (ChocoVision, UK). The temperature was increased from 20 to 45 $°C$ in order to melt all the cocoa butter crystals and then gradually cooled down to the desired nozzle temperature. The sample temperature was measured using a thermocouple and kept constant before every test was performed.

2.2. Chocolate Characterization

2.2.1. Differential Scanning Calorimetry (DSC)

The thermal behaviour of the chocolate was characterized using a DSC Q2000 (TA Instruments, UK). Samples were loaded into sealed pans, heated up from 20 $°C$ to 45 $°C$ at a temperature rate of 3 $°C/min$ in order to melt all the cocoa butter crystals and subsequently cooled down to 0 $°C$ at the same rate. Each test was repeated in duplicate.

2.2.2. Rheological Characterization

The rheological characterization of the chocolate was performed using a Paar-Physica UDS2000 rotational rheometer equipped with a cone and plate geometry (d = 23 mm ; $\theta = 2°$), at a 50 μm minimum gap. Chocolate viscosity was measured varying the shear rate between 1 and 60 s^{-1}. This range was selected based on the theoretical predictions of the capillary flow into the Printer nozzle ($d_n = 0.8$ mm). The chocolate was tested at respectively 26 and 32 $°C$. Each measurement was repeated in triplicate.

2.3. Print Geometry

A customized *"wall geometry"*, consisting of 16 7 cm-long layers deposited on the top of each other was specifically designed for this study. The layer thickness, h_{layer}, was kept constant at 0.6 mm. A 2D sketch of the CAD geometry is reported in figure 1 (b).

2.4. Paste Extrusion 3D Printing

A Paste Extrusion 3D Printer, Choc Creator V2.0 Plus (Choc Edge Ltd, UK), shown in Fig. 1, was used to manufacture 3D structures by deposition of thin layers of chocolate from a heated nozzle onto a build plate. The molten chocolate was loaded directly from the tempering machine into a heated steel syringe with a 0.8 mm nozzle and loaded into the print head.

3D structures were designed using FreeCAD software. The stereolithography file (.stl) was subsequently imported in the printer Slicer software were the printing parameters have been set and a G-code automatically generated. The 3D printer Slicer divides the geometry in several layers and split the process in a series of elementary movements where the geometrical coordinates and the amount of material extruded are defined. In particular, as shown in figure 1 (a), in the 3D printer considered in this study, the printing head is able to move along the y-z axes, whereas the building plate can move along the x- axis. The displacement of the syringe plunger regulates the flow through the nozzle.

In this study, chocolate was extruded from the heated nozzle when it moved from $y = 0$ to $y = L$ at the printing velocity V_p; whereas the print head translated without extruding in the opposite direction at a set travel velocity V_t, from $y = L$ to $y = 0$. Printing conditions were varied systematically to understand their effect on the heat transfer. In particular, the effect of printing velocity V_p and the build plate temperature, T_e, were studied as summarised in table 1. The travel velocity, V_t, was set to 8 mm/s for the lowest two printing velocities and to 12 mm/s for the highest printing velocities.

Table 1: Experimental printing condition.

Parameter	Range
$T_n \quad [^\circ C]$	32
$T_e \quad [^\circ C]$	[18, 20, 22]
$V_p \quad [mm/s]$	[4, 8, 12, 16]
$V_t \quad [mm/s]$	[8, 8, 12, 12]

2.5. IR Thermography

An IR Camera Testo 885 (S.A. Testo N.V, Belgium) was used to measure the temperature profiles of the deposited chocolate, during deposition onto the build plate. The camera was placed in front of the build plate, focusing on the y-z axis (Fig. 1 (a)). Videos were recorded during the all duration of the experiment, at 320x240 pixel resolution and a frame rate of 33 Hz. The green line in figure 1 (b) represents the region where the temperature of the chocolate was measured just before the collapse. The height of the structure was measured over time from the video using image analysis via the ImageJ software. Every test was repeat at least three times.

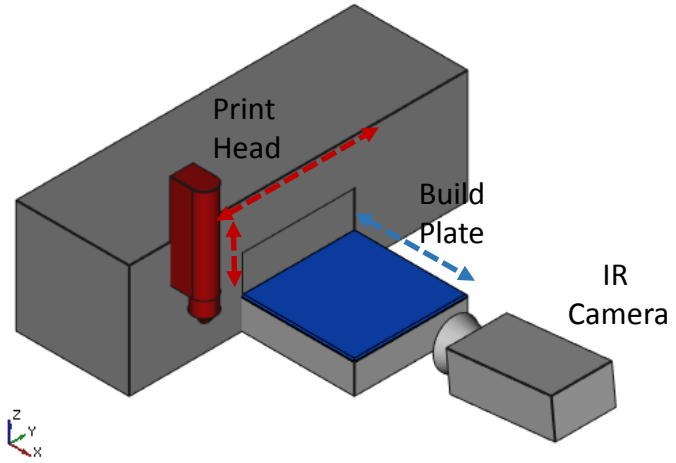

(a) *Schematics of the ChocEdge 3D Printer: the build plate (blue) is kept a constant temperature (T_e) and moves along the x-axis; whereas the print head (red) is heated at a temperature (T_n) and it moves along the y-z axes.*

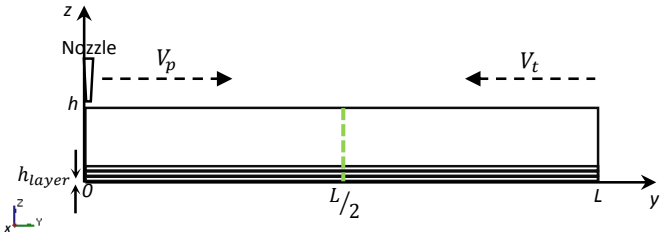

(b) *2D Sketch of the printed structure with its dimensions respectively 7 cm length and 1 cm height. The layer thickness, h_{layer}, is equal 0.6 mm. The green line highlight the region where the temperature has been measured in fig. 5.*

Figure 1: *Scheme of the experimental apparatus set-up.*

3. Results and Discussion

The material properties will be presented first, followed by the thermal characterization performed to investigate the heat transfer after deposition. A simple theory is proposed to link the product rheological properties, its cooling dynamics and the print stability or its collapse.

3.1. Chocolate Characterisation

In figure 2 are reported the heat flow curves of the chocolate, measured using the DSC. During the heating step the heat flow drastically decreases when the temperature is increased above 29 $°C$, showing an endothermic transition, which indicates the melting of the cocoa butter crystals. It is possible to observe a peak at 33.38 $°C$, showing that cocoa butter crystals were present in the V form [18]. Conversely, during the cooling step, it is possible to see an exothermic transition, between 24 and 0 $°C$ with a peak at a temperature 14.35 $°C$. The enthalpy of crystallization ΔH_{cryst}, calculated from the integral of the exothermic transition, was found to be 45.78 J/g; the specific value of enthalpy of crystallization per gram of cocoa butter was found equal to 121.11 J/g_{CB}, this value represent the energy per gram that the cocoa butter releases during the crystallization. The crystallization enthalpy measured in this study is slightly higher compared to the values reported in [24], where it varies from 83 to 100 J/g_{CB} , probably due to a different protocol.

The shear viscosity and flow curves of the chocolate at different temperature are reported respectively in figures 3 (a), (b). At every temperature, the viscosity decreases when the shear rate is increased; showing a shear-thinning behaviour.

The shear-thinning behaviour of chocolate is well known in the literature ([18], [21]). This is a desirable feature in extrusion 3D printing processes, where the printing material is subject to higher stress during the extrusion from the nozzle and their lower viscosity guarantees an easy flowability [8]. On the other hand, the higher viscosity at low shear rate after deposition helps printed structures to hold their shape. It was found that the experimental mass flow rate ($\dot{m}_{Exp}$), increases linearly with the printing velocity. Its value was slightly higher compared to the theoretical prediction and can be estimated as $\dot{m}_{Exp} = k_1 \cdot \dot{m}_{theo} = k_1 \cdot \frac{\pi d_n^2}{4} V_p \rho$; where $k_1 = 1.12$.

At a temperature of 32 $°C$, chocolate viscosity varies between 32 to 3 $Pa \cdot s$, depending on the shear rate; whereas the shear stress varies between 35 and 180 Pa. The cocoa butter is still liquid, in agreement to the DSC cooling curves. On the other hand, at a temperature of 26 $°C$, chocolate is more viscous because cocoa butter begins to form crystals, increasing the solid fraction of the suspension and therefore its viscosity. Moreover, the standard deviations are slightly higher, showing a higher variability due to the presence of cocoa butter crystals. At lower temperatures, the cocoa butter solidified during the rheological tests, making impossible to measure the material rheology. Similar results were presented by Mantihal *et al.* [9], who investigated temperature ramp on chocolate samples to characterize thermal and flow properties for the

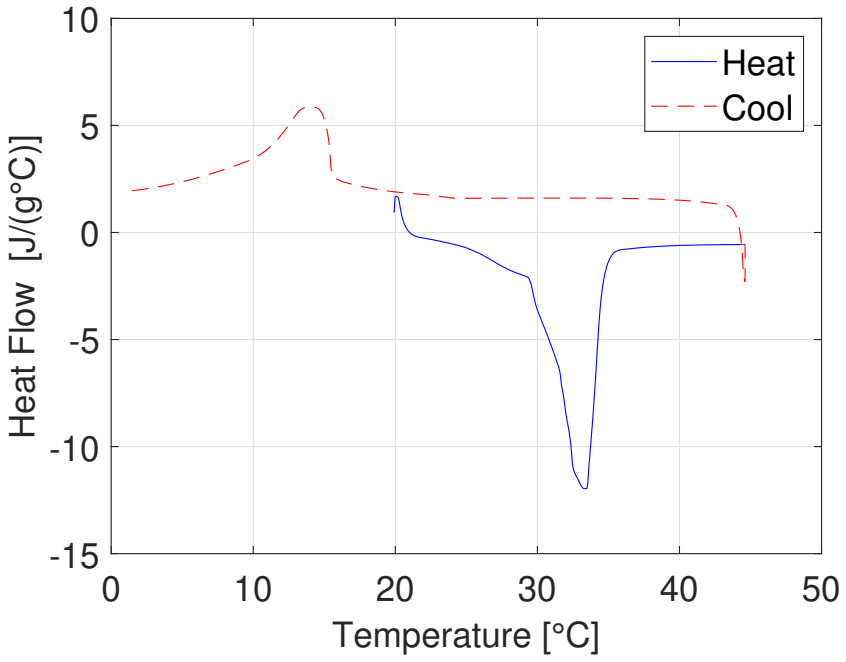

Figure 2: *DSC Heat Flow Curves: initially the chocolate has been heated from 20 to 45 °C (blue continuous line), the temperature has been subsequently decreased to 0 °C (red dotted line.)*

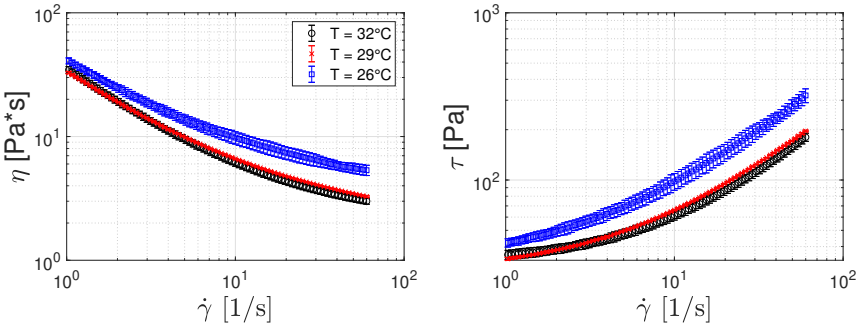

(a) *Viscosity, η, versus shear rate, $\dot{\gamma}$* (b) *Shear stress, τ, versus shear rate, $\dot{\gamma}$*

Figure 3: *Flow curves of chocolate at different temperature: $T = 32$ °C (black dots), $T = 29$ °C (red cross) $T = 26$ °C (blue squares).*

3D printing of chocolate. However, the chocolate used in that study had a lower cocoa butter content (63.5% solids' content and 33% cocoa butter) and crystallized between 29 and 32 $°C$.

To determine the chocolate yield stress at different temperatures, the shear stress results were fitted with the Herschel-Bulkley model (Eq. 1) [21], using Matlab, considering a non-linear-square method (with 95% of confidence on bounds).

$$\begin{cases} \tau < \tau_0, & \dot{\gamma} = 0 \\ \tau > \tau_0, & \tau = \tau_0 + K\dot{\gamma}^n \end{cases} \tag{1}$$

The model's parameters are the yield stress τ_0, the consistency index K and the flow index n. This model used to describe chocolate steady shear flow curve by Sokmen *et al.*, as alternative to the Casson model [21]. The material behaves as a solid if the stresses applied are lower than the yield stress, otherwise it flows, following a power law behaviour. Chocolate's fitting parameters at different temperatures are summarized in table 2.

Table 2: Rheological parameters obtained from the Herschel-Bulkley fitting of chocolate.

$T[°C]$	$\tau_0[Pa]$	$K[Pa \cdot s^n]$	n	R^2
26	38.28	7.17	0.9	0.9987
29	31.31	4.50	0.9	0.9992
32	31.75	3.38	0.9	0.9894

The Herschel-Bulkley model with $n = 0.9$ provided a good agreement with experiments, as shown from the values of the R^2. The yield stress and K were significantly higher at 26 $°C$, consistently with the expected higher fat solid fraction in the chocolate.

3.2. Structure Collapse

The effect of the different operating conditions on the heat transfer will be presented in the following paragraph to understand the causes of the collapse observed in some experimental conditions.

Printing velocity and build plate temperature both affect the chocolate cooling dynamics and ultimately also the structure stability. Different combinations of these two parameters have been considered. As summarized in figure 4, three different *"regimes"* were identified: stable structures (green), collapse (orange) and material dripping followed by a collapse (red). In particular, it was possible to successfully print structures at a T_e equal to 18 $°C$ and a printing speeds lower than $16mm/s$ (from 4 to 12 mm/s) and at a T_e equal to 20 $°C$ and a V_p of 4 mm/s; whereas at higher printing speeds and environmental temperature the cocoa butter does not have enough time to crystallize leading to a collapse of the structure. Finally, at T_e of 22 $°C$ and V_p between 8 and 12 mm/s, during the layer deposition occurs dripping of liquid chocolate from the nozzle, followed by the collapse of the structures.

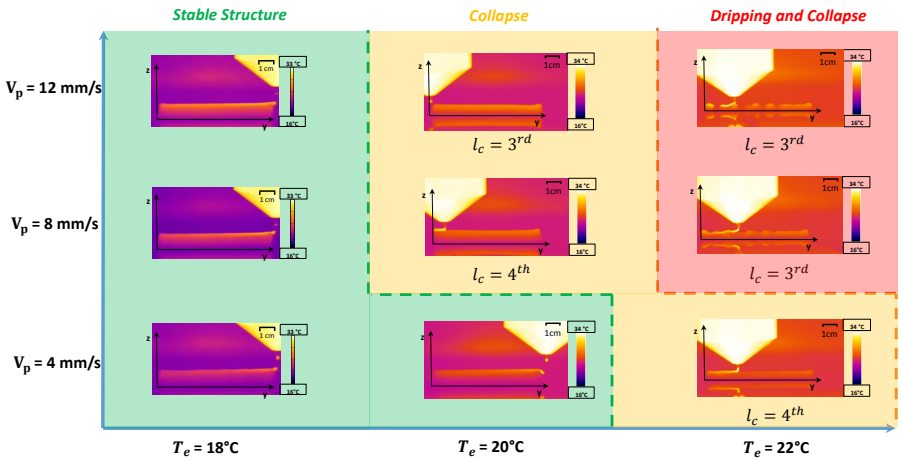

Figure 4: *3D print stability map at different combinations of Environmental Temperature (T_e) and Printing Velocity (V_p). The images show the structure at the end of the printing or just before collapsing; the collapse's layer (l_c) is reported in case of collapse. Collapse is always observed when $V_p = 16mm/s$*

In an extrusion-based 3D printing process, structures are created adding several layers that bond together. The bottom layers have to support the weight of the upper layers without deforming to avoid collapse. In this paragraph we present a simple theory to describe the conditions leading to a stable structure or to a collapse. In particular, we define the maximum theoretical structure height:

$$H_y = \frac{\tau_0}{\rho g} \tag{2}$$

where τ_0 is the yield stress, ρ and g are respectively the chocolate's density and the gravitational acceleration. We propose that until the printed chocolate has solidified, for print stability to be guaranteed, everywhere in the structure the yield stress should be higher than stress imposed from the weight of the upper layers. Given that the yield stress of the chocolate suspension depends on its temperature, the cooling dynamics conditions strongly the print stability. At a given temperature, a printed structure is stable only if its height is lower than the maximum theoretical structure height introduced above.

In food 3D printing, Liu *et al.* tried to correlate the structure stability to the values of the yield stress, storage and loss modulus of the printing material and the room temperature [14]. However, in that study, it was investigated the 3D printing of gel suspensions, made of k-carrageenan, xanthan gum and potato starch, which have a yield stress higher than 1000 Pa at a temperature of 25 $°C$. The yield stress of chocolate increases when the temperature drops

below 26°C and even more drastically below 24 °C, due to the cocoa butter crystallization. Lanaro *et al.* [23] estimate a yield stress of 14 $Pa \cdot s$ of a dark chocolate formulation at temperatures between 30 °C at low shear rates. However, the rheology at this temperature is still too high for understanding the material behaviour after deposition.

In figure 5 (a) we presented a typical IR image showing the temperature distribution of the printed structure just before its collapse. It is possible to identify a region at the base where the temperature of the chocolate is lower than 24 °C and thus partially crystallized. Analysing the structure collapse, it was found that the structures yield and fall, depending on the printing condition, along the third or forth layer. Moreover, even along the same layer, it is possible to identify regions where the measured temperature profiles vary due to different local heat transfer coefficient. In particular, at the center of the structure ($y = L/2$) the temperature is slightly higher compared to the structure's edges ($y = [0, L]$), presumably due to a lower local air temperature due to boundary effects. These differences in the local heat transfer could justify why the collapse is typically starting around $y = L/2$.

Table 3: Printing conditions leading to the 3D printed structure collapse and the conditions measured just before collapse: temperature, T_c, height, h_c, and time, t_c.

T_e [°C]	V_p [mm/s]	T_c [°C]	h_c [mm]	t_c [s]
18	16	25.0 ± 0.4	2.25 ± 1.1	121.0 ± 15.27
20	8	24.7 ± 0.1	2.69 ± 0.4	245.0 ± 6.1
	12	25.6 ± 0.2	2.07 ± 0.3	160.4 ± 2.1
22	4	26.5 ± 0.3	2.84 ± 0.1	183.7 ± 6.3
	8	26.4 ± 0.2	1.80 ± 0.1	52.5 ± 0.7
	12	26.9 ± 0.3	1.80 ± 0.1	43.7 ± 4.1

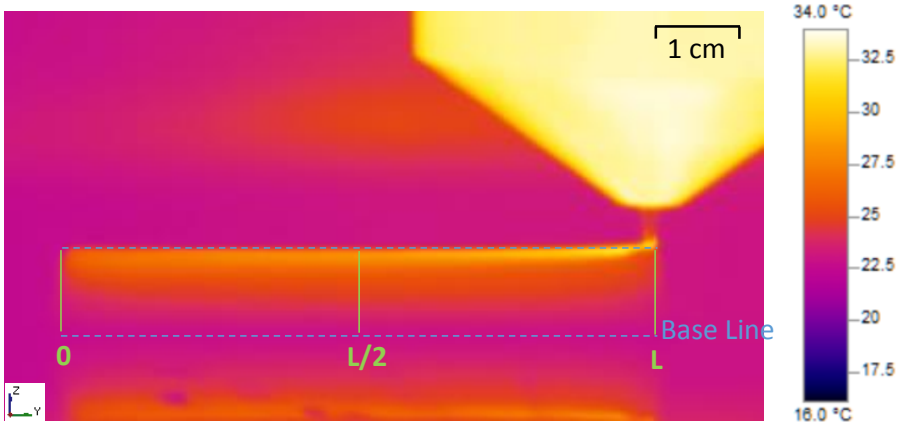

(a) *Sketch of Chocolate Temperatures Profiles measured along the z-axis.*

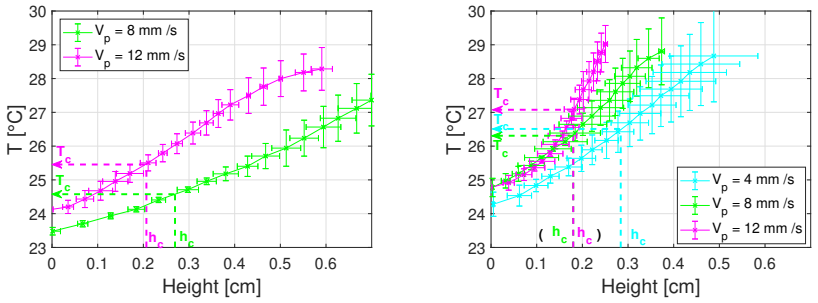

(b) $T_e = 20\ °C$. (c) $T_e = 22\ °C$.

Figure 5: *Temperature distribution of the printed structure just before the collapse at $L/2$ for different environmental temperature and printing velocity respectively: $V_p = 4$ mm/s (cyan), $V_p = 8$ mm/s (green), $V_p = 12$ mm/s (magenta).*

In order to investigate the causes leading to a structure collapse, the temperatures profiles along the z-axis of the 3D structures have been measured at $y = L/2$ right before the instant of collapse. Results are reported in figures 5 (b), (c) for different environmental temperature (T_e). The temperature increased along the height of the structure (z), since the chocolate at the top was deposited later. For a given T_e, a higher V_p led to higher temperatures since the chocolate had less time to cool down when a higher printing speed was used. For each curve, the temperature of collapse, T_c, has been measured from the IR images at the height at which the collapse occurs, h_c and at the time of collapse t_c. These quantities have been reported in table 3 and depend on the printing velocity and environmental temperature. In general, decreasing V_p increases the cooling rate and allows building taller structures. Also the collapse temperature T_c is higher at higher T_e and V_p, with the only exception of the structure printed at $T_e = 22°C$ and $V_p = 4mm/s$.

Figure 6 (a) summarizes in a histogram the temperature of the layer at which the structures collapse. The red dotted line represents the temperature of $26°C$ below which the rheological properties suggest a progressive solidification and at which H_y is computed. Furthermore, figures 6 (b), (c), (d) show a comparison between the evolution of the experimental and the theoretical structure heights. The addition of each layer increases step-wise the overall height of Δh. The frequency at which the stresses increases depends from the printing and travelling velocities. In particular, increasing the printing velocity decreases the overall printing time of the 3D structure and decreases the cooling time of the deposited chocolate. At each printing condition, the additional height is estimated by taking as a reference (i.e. on top of) the layer along which the structure is observed to collapse.

The structural collapses occur at the third or fourth layers because the bottom cools more rapidly thanks to the proximity with the heat conductive printing plate. It was possible to identify two different collapse dynamics: at a T_e of 18 and 20 $°C$, when the printing speed is too high, the collapse occurs in few seconds due to the deposition of an excess of chocolate on the vertical axes, which suddenly increases the stress acting on the lower layers. On the other hand, at a T_e of 22 $°C$ the deposited chocolate slowly flows while on the plate, increasing the gap between the nozzle height and the printed layer. The gap begins to increase after the deposition of the sixth layer and, probably due to the high environmental temperature slowing down the cocoa butter crystallization.

Figure 6 (b) shows that the progression of the structure height for T_e= 20 $°C$. In this case, the measured height matches perfectly the values of the theoretical values until the structure rapidly collapses. The measured height on the structures exceeds the value of H_y estimated from the measured yield stress at 26 $°C$. However, comparing the temperature with the measured T_c it is possible to notice that those values are between 24.5 and 25.5 $°C$ meaning that the deposited chocolate has partially crystallized, increasing significantly the value of the yield stress. The yield criterion cannot be tested quantitatively for those conditions since the yield stress could not be measured at temperature lower than 26 $°C$.

Figures 6 (c), (d) describe the collapses observed at a $T_e = 22°C$. In this case it is possible to observe that the values of the measured heights are slightly lower compared to the values of the theoretical values, meaning that the printed material slowly begins to flow after the deposition. Ultimately, when the H_{EXP} exceeds the values of H_y, estimated form the yield stress at 26 $°C$, the structure collapses, in agreement to the yield criterion proposed in Eq.2.

4. Conclusions

In this study, we have investigated the effect of process conditions and rheological and heat transfer properties of a dark chocolate on the print stability, during paste extrusion 3D printing. IR Thermography has been successfully used as a non-invasive technique to measure the local temperature evolution, during 3D printing. Chocolate 3D structures were successfully manufactured

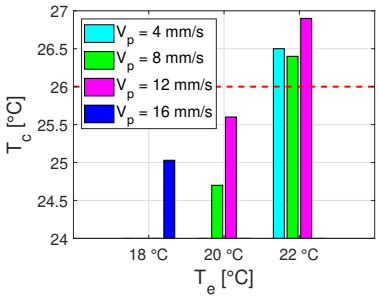

(a) *Temperature of the collapsing layer T_c, measured at the time of collapse, t_c at $y = L/2$*

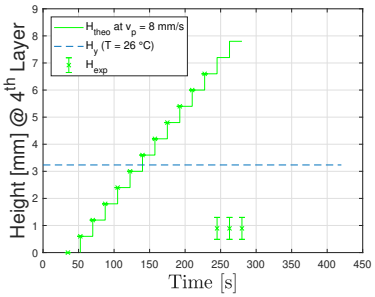

(b) *Additional height above the forth layer at $T_e = 20°C$.*

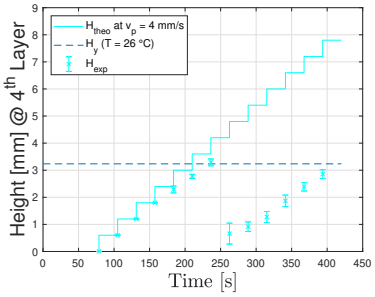

(c) *Additional height above the third layer at $T_e = 22°C$.*

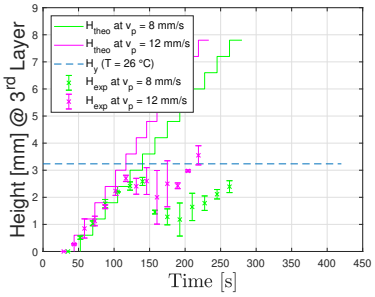

(d) *Additional height above the forth layer at $T_e = 22°C$.*

Figure 6: *Comparison between theoretical (continuous line) and experimental height (cross dots), above the collapse layer during printing. The maximum height H_y (dotted line) at different environmental temperature T_e and printing velocity: $V_p = 4$ mm/s (cyan), $V_p = 8$ mm/s (green), $V_p = 12$ mm/s (magenta).*

at a T_e of 18 $^\circ C$ using a range of printing velocity between 4 and 12 mm/s; whereas at T_e of 20 $^\circ C$, only V_p equal to 4 mm/s led to stable structures.

Experimental results show that the material temperature after deposition was mainly affected by the environmental air, build plate temperature and printing velocity. In order to successfully manufacture 3D structures, the cooling of the printing material should guarantee that, before the chocolate solidifies, the yield stress in every part of the structure is higher than the stress applied from the layers above. The printing conditions, in particular printing velocity and environmental temperature, should be chosen in order to guarantee that the cocoa butter has enough time to solidify.

The results presented in this article and the novel approach proposed can be useful to optimize the printing condition, based on the heat and rheological properties of food products undergoing a sharp rheological transition upon cooling. Interesting directions for future research include extending this approach to complex geometries and furthering the understanding of the sintering dynamics between the layers, which can influence the mechanical and textural properties of the printed food.

5. Acknowledgments

The authors would like to thank Prof. Joe Keddie, Gareth Coffin and Sadie Fleetwood for the fruitful discussions and Violeta Doukova for the technical support.

References

[1] J. Sun, W. Zhou, D. Huang, J.Y.H. Fuh, G. Soon Hong, *An overview of 3D printing technologies for food fabrication*, Food Bioprocess Technology, 8(8) (2015), pp. 1605-1615.

[2] F.C. Godoi, S. Prakash, B.R. Bhandari, *3D printing technologies applied for food design: Status and prospects*, Journal of Food Engineering, 179 (2016), pp. 44-54.

[3] B.N. Turner, R. Strong, S.A. Gold, *A review of melt extrusion additive manufacturing processes: I. Process design and modeling*, Rapid Prototyping Journal, 20 (2014), pp. 192-204.

[4] Q. Sun, G.M. Rizvi, C.T. Bellehumeur, P. Gu, *Effect of processing conditions on the bonding quality of FDM polymer filaments*, Rapid Prototyping Journal, 14(2) (2008), pp. 72-80.

[5] C. Bellehumeur , L. Li, Q. Sun , P .Gu, *Modeling of Bond Formation Between Polymer Filaments in the Fused Deposition Modeling Process*, Journal of Manufacturing Processes, 6(2) (2004), pp. 170-178.

[6] J.E. Seppala, K.D. Migler, *Infrared thermography of welding zones produced by polymer extrusion additive manufacturing*, Additive Manufacturing, 12 (2016), pp. 71–76.

[7] H. Chen, F. Xie, L. Chen, Z. Bo, *Effect of rheological properties of potato, rice and corn starches on their hot- extrusion 3D printing behaviors*, Journal of Food Engineering, 244 (2019), pp. 150–158.

[8] Z. Liu, M. Zhang, B. Bhadari, C. Yang, *Impact of Rheological Properties of Mash Potatos on 3D Printing*, Journal of Food Engineering, 220 (2018), pp. 1-7.

[9] S. Mantihal, S. Prakash, F.C. Godoi, B. Bhandari, *Optimization of chocolate 3D printing by correlating thermal and flow properties with 3D structure modeling*, Innovative Food Science and Emerging Technologies, 44 (2017), pp. 21–29.

[10] S. Mantihal, S. Prakash, B. Bhandari, *Textural modification of 3D printed dark chocolate by varying internal infill structure*, Food Research International, 121 (2019), pp. 648 - 657.

[11] V. Vancauwenberghe, L. Katalagarianakis, Z. Wang, M. Meerts, M. Hertog, P. Verboven, P. Moldenaers, M.E. Hendrickx, J. Lammertyn, B. Nicolai, *Pectin based food-ink formulations for 3D printing of customizable porous food simulants*, Innovative Food Science & Emerging Technologies, 42 (2017), pp. 138 - 150.

[12] L. Wang, M. Zhang, B. Bhandari, C. Yang, *Investigation on fish surimi gel as promising food material for 3D printing*, Journal of Food Engineering, 220 (2018), pp. 101-108.

[13] F. Yang, M. Zhang, B. Bhandari, Y. Liu, *Investigation on lemon juice gel as food material for 3D printing and optimization of printing parameters*, LWT - Food Science and Technology, 87 (2018), pp. 67-76.

[14] Z. Liu, B. Bhandari, S. Prakash, S. Mantihal, M. Zhang, *Linking rheology and printability of a multicomponent gel system of carrageenan-xanthan-starch in extrusion based additive manufacturing*, Food Hydrocolloids, 87 (2019), pp. 413–424.

[15] M.A.I. Schutyser, S. Houlder, M. de Wit , C.A.P. Buijsse , A.C. Alting, *Fused deposition modelling of sodium caseinate dispersions*, Journal of Food Engineering, 220 (2018), pp. 49-55.

[16] A. Derossi, R. Caporizzi, D. Azzollini, C. Severini, *Application of 3D printing for customized food. A case on the development of a fruit-based snack for children*, Journal of Food Engineering, 220 (2018), pp. 65-75.

[17] C. Severini, A. Derossi, I. Ricci, R. Caporizzi, A. Fiore, *Printing a blend of fruit and vegetables. New advances on critical variables and shelf life of 3D edible objects*, Journal of Food Engineering, 220 (2018), pp. 89 -100.

[18] S.T. Beckett, *Industrial Chocolate Manufacture and Use*, Wiley-Blackwell 4th ed. (2009), pp. 224-246.

[19] V. Glicerina, F. Balestra, M. Dalla Rosa, S. Romani, *Microstructural and rheological characteristics of dark, milk and white chocolate: A comparative study*, Journal of Food Engineering, 169 (2016), pp. 165-171.

[20] E.O. Afoakwa, A. Paterson, M. Fowler, J. Vieira, *Relationship between rheological, textural and melting properties of dark chocolate as influenced by particle size distribution and composition*, European Food Research Technology, 227 (2008), pp. 1215-1223.

[21] A. Sokmen, G. Gunes, *Influence of some bulk sweeteners on rheological properties of chocolate*, LWT - Food Science and Technology, 39 (2006), pp. 1053–1058.

[22] L. Hao, S. Mellor, O. Seaman, J. Henderson, N. Sewell , M. Sloan, *Material characterisation and process development for chocolate additive layer manufacturing*, Virtual and Physical Prototyping, 5(2) (2010), pp. 57-64.

[23] M. Lanaro, D.P. Forrestal, S. Scheurer, D.J. Slinger, S. Liao, S.K. Powell, M.A. Woodruff, *3D printing complex chocolate objects: Platform design, optimization and evaluation*, Journal of Food Engineering, 215 (2017), pp. 13-22.

[24] J.S. Aronhime, S. Sarig, N. Garti, *Reconsideration of polymorphic transformations in cocoa butter using the DSC*, Journal of the American Oil Chemists' Society, 65(7) (1988), pp. 1140-1143.